Geochemistry, Geophysics, Geosystems

RESEARCH ARTICLE
10.1029/2019GC008267

Key Points:
- IODP Site U1438 records a unique 4-Ma history of rhyolite eruptions from the Kyushu-Ryukyu arc
- Explosive (>6 M) eruptions at 4 Ma, 2–2.5 Ma and <1 Ma in southwest Japan recorded in deep ocean basin (Amami-Sankaku Basin)
- Radiogenic isotopes of tephra might be key to distinguish the source of eruptive products

Supporting Information:
- Supporting Information S1
- Table S1
- Table S2

Correspondence to:
A. McCarthy,
anders.mccarthy@bristol.ac.uk

Citation:
McCarthy, A., Yogodzinski, G., Tepley, F. J., III, Bizimis, M., Arculus, R., & Ishizuka, O. (2019). Isotopic characteristics of Neogene-Quaternary tephra from IODP Site U1438: A record of explosive volcanic activity in the Kyushu-Ryukyu arc. *Geochemistry, Geophysics, Geosystems*, *20*, 2318–2333. https://doi.org/10.1029/2019GC008267

Received 11 FEB 2019
Accepted 13 APR 2019
Accepted article online 23 APR 2019
Published online 16 MAY 2019

Isotopic Characteristics of Neogene-Quaternary Tephra From IODP Site U1438: A Record of Explosive Volcanic Activity in the Kyushu-Ryukyu Arc

Anders McCarthy[1,2], Gene Yogodzinski[3], Frank J. Tepley III[4], Michael Bizimis[3], Richard Arculus[5], and Osamu Ishizuka[6,7]

[1]Institute of Earth Sciences, University of Lausanne, Lausanne, Switzerland, [2]Now at School of Earth Sciences, University of Bristol, Bristol, UK, [3]School of Earth, Ocean, and Environment, University of South Carolina, Columbia, SC, USA, [4]College of Earth, Ocean and Atmospheric Sciences, Oregon State University, Corvallis, OR, USA, [5]Research School of Earth Sciences, Australian National University, Canberra, ACT, Australia, [6]Geological Survey of Japan/AIST, Tsukuba, Japan, [7]Research and Development Center for Ocean Drilling Science, Japan Agency for Marine-Earth Science and Technology, Yokosuka, Japan

Abstract International Ocean Discovery program (IODP) Site U1438 is located within the Amami-Sankaku Basin, ~50 km SW of the Kyushu-Palau Ridge and ~500 km SE of the present-day volcanic front of the Kyushu-Ryukyu arc. Thirty-eight rhyolitic tephra layers (1–15 cm thick) deposited over the last 4 Myr were recovered at this site. Representative ash layers dominated by unaltered, colorless glass shards reaching 100–300 μm in size, in association with rare pyroxene, amphibole, biotite, and zircon, were sampled for isotopic analysis. The isotopic compositions of the tephra have a narrow range in $^{87}Sr/^{86}Sr$ (0.704 to 0.706), $^{206}Pb/^{204}Pb$ (18.32 to 18.46), $^{207}Pb/^{204}Pb$ (15.57 to 15.62), and $^{208}Pb/^{204}Pb$ (38.46 to 38.75) and are more variable in ε_{Nd} (−3.5 to +4.8) and ε_{Hf} (+2.0 to +13.3). This record indicates the tephra were not sourced from the Izu-Bonin-Mariana arc or from Central Japan but derived from felsic volcanism from the Kyushu-Ryukyu arc. The 4.8-km-deep Amami-Sankaku Basin was located up to 600–900 km from the Kyushu-Ryukyu arc over the last 4 Ma, which is significantly more distal than other drill sites from which extensive tephra layers sourced from SW Japan have been recovered. Site U1438 tephra are thus likely related to widely distributed ($M > 6$) rhyolitic eruptions. We propose the unique tephra record and high-precision isotope analysis of recovered tephra from Site U1438 can be used as an important marker to identify submerged calderas within the Ryukyu arc and/or constrain the history of activity (>1 Ma) of major calderas-forming eruptions within the Kyushu-Ryukyu arc.

1. Introduction

Large caldera-forming eruptions are regional and global hazards and may act as an important control on short- and long-term climate change (e.g., Self, 2006). This is particularly the case in Japan where the historical and geological records shows periods of intense volcanism associated with caldera-forming, explosive rhyolitic eruptions (e.g., Machida, 1999, 2002; Yamamoto et al., 2018). The historical tephra record is thus of fundamental importance in any effort to build a comprehensive representation of the explosive volcanic activity through time of particular arc segments in order to better mitigate potential volcanic hazards (e.g., Self, 2006) and constrain the long- and short-term tectonic, mantle and subduction control on timescales of magma production and volcanism (e.g., DeCelles et al., 2009; Ducea et al., 2015; Kimura et al., 2014).

Tephra recovered from ocean sediments are an important resource aiding the completion of tephra records developed through on-land studies (e.g., Kutterolf et al., 2018; Schindlbeck et al., 2018, and references therein). Subaerial tephra records are typically more prone to erosion, burial, and alteration, particularly for older sequences, and so are often less complete (e.g., Mahony et al., 2016). Moreover, subaerial tephra deposits might also reflect the effects of more local eruptions whose effects are negligible at the larger (e.g., Japan) scale (e.g., Torii et al., 2000). Correlations between individual tephra layers over several hundreds of kilometers in both marine and subaerial settings are also hampered by uncertainties in chronology, postdepositional erosion, bioturbation and localized versus regional tephra fallout (e.g., Mahony et al., 2016). Though individual tephra layers might be correlated through depositional ages, the mineralogy and composition of glass shards is crucial in determining their sources (e.g., Kotaki et al., 2011; Schindlbeck et al., 2018; Tsuji et al., 2017). Nevertheless, constraining the source and extent of ash

deposits is an ongoing challenge, as tephra deposits may also derive from currently unknown volcanic sources, such as submerged calderas (e.g., Tatsumi et al., 2018), volcanic centers covered by products of younger eruptions, or might be related to calderas with unconstrained ages, or whose relations with particular tephra markers are disputed (e.g., Moriwaki et al., 2008; Nishizawa & Suzuki, 2016).

The Quaternary tephrostatigraphy of Japan, based on the detailed study of sedimentary basins and Ocean Drilling Program (ODP)/Deep Sea Drilling Project/International Ocean Discovery program (IODP) stratigraphy and samples, is well established. Consequently, the timing of recent silicic, caldera-forming eruptions, which cover parts of Japan in thick deposits, is relatively well known (e.g., Kimura et al., 2015; Machida, 1999, 2002). Though source characterization and correlations of large-scale rhyolitic eruptions in the last 5 Ma have been recently attempted using Pb isotope composition of glass shards (Kimura et al., 2015), the tephrostratigraphy and locations of caldera-forming eruptions older than 1 Ma in Japan remains significantly less well constrained (e.g., Mahony et al., 2016).

In order to determine more precisely the extent and volumes of tephra fallout related to large-scale eruptions >1 Ma, it is necessary to target tephra layers from ocean basins hundreds of kilometers from any arc-front or (known) volcanic source. This paper reports new isotopic data (Sr-Nd-Hf-Pb) for 17 rhyolitic tephra layers younger than <4 Ma and one older tephra layer (ca. 14 Ma) sampled during IODP Expedition 351 from a deep ocean basin SE of Kyushu. On the basis of comparisons with existing data for tephra of known provenance, we conclude that rhyolitic tephra from the Amami-Sankaku Basin (ASB) were derived from previously unrecognized and major eruptive sources in the Kyushu-Ryukyu arc. The tephra record of the ASB might therefore be used as markers to extend the record of major caldera-forming eruptions in southwest Japan beyond 1 Ma.

2. Background

In 2014, IODP Expedition 351 targeted Site U1438 within the ASB (4.8 km below sea level) in the north central portion of the Philippine Sea plate (Figure 1). The basin is located ~50 km SW of the Kyushu-Palau Ridge (KPR), a remnant of subduction at the Izu-Bonin-Mariana (IBM) Arc that was created between 50 and 25 Ma (e.g., Arculus et al., 2015; Ishizuka et al., 2011). The ASB is located ~500 km SE of the present-day volcanic front of the Kyushu-Ryukyu arc, ~850 km south of the Southwest Japan arc (e.g., Kamata & Kodama, 1999), and ~640 km west of the currently active Izu-Bonin arc (Figure 1). The formation of the Southwest Japan and Kyushu-Ryukyu arcs results from the subduction of the Philippine Sea plate beneath southwestern Japan. Variations in magmatism over the last 15 Ma reflect changes in subduction dynamics, including changes in orientation of subduction in Pleistocene-Pliocene times, subduction of the KPR and Shikoku Basin (e.g., Kamata & Kodama, 1999; Kimura et al., 2014; Mahony et al., 2016; Pownall et al., 2017; Shinjo et al., 2000).

One of the primary aims of IODP Expedition 351 was to target the sedimentary and volcaniclastic record at Site U1438 to constrain the evolution of the arc following inception at ~50 Ma (Arculus et al., 2015). Sediments and sedimentary rocks recovered at Site U1438 up to 1461 m below seafloor (mbsf) were separated into four distinct lithostratigraphic units (Units I to IV; Arculus et al., 2015) and overly a unit of igneous basement (Unit 1: 1461–1611 mbsf). The deeper portions of the volcaniclastic and sedimentary record in the core (Unit III: ~310–1361 mbsf, and IV: ~1361–1461 mbsf) are primarily related to the Paleogene Izu-Bonin arc developed at the KPR (50 to 25 Ma; Brandl et al., 2017). These 1,300 m of volcaniclastic gravity flow deposits (tuffaceous mudstones, tuffaceous sandstones, and tuffaceous breccia-conglomerates) overlie an igneous basement of low-Ti, low-K tholeiitic basaltic lava flows of 49.3- to 46.8-Ma age (Ishizuka et al., 2018). The uppermost 160.3 m (Unit I) of the ASB sediments, however, comprise tuffaceous mud and mud with ash containing occasional centimeter-thick ash layers (Figures 2a and 2b). The pelagic sediments of Unit I were deposited at low rates consequent to the cessation of volcanism and magmatic activity of the KPR at circa 25 Ma (Arculus et al., 2015).

3. Samples and Methods

Tephra layers recovered in Unit I were identified during shipboard core description on IODP Expedition 351 using standard description methods, including smear-slides, changes in sediment color, magnetic susceptibility, and grain size. The presence and thickness of individual layers was then double-checked onshore

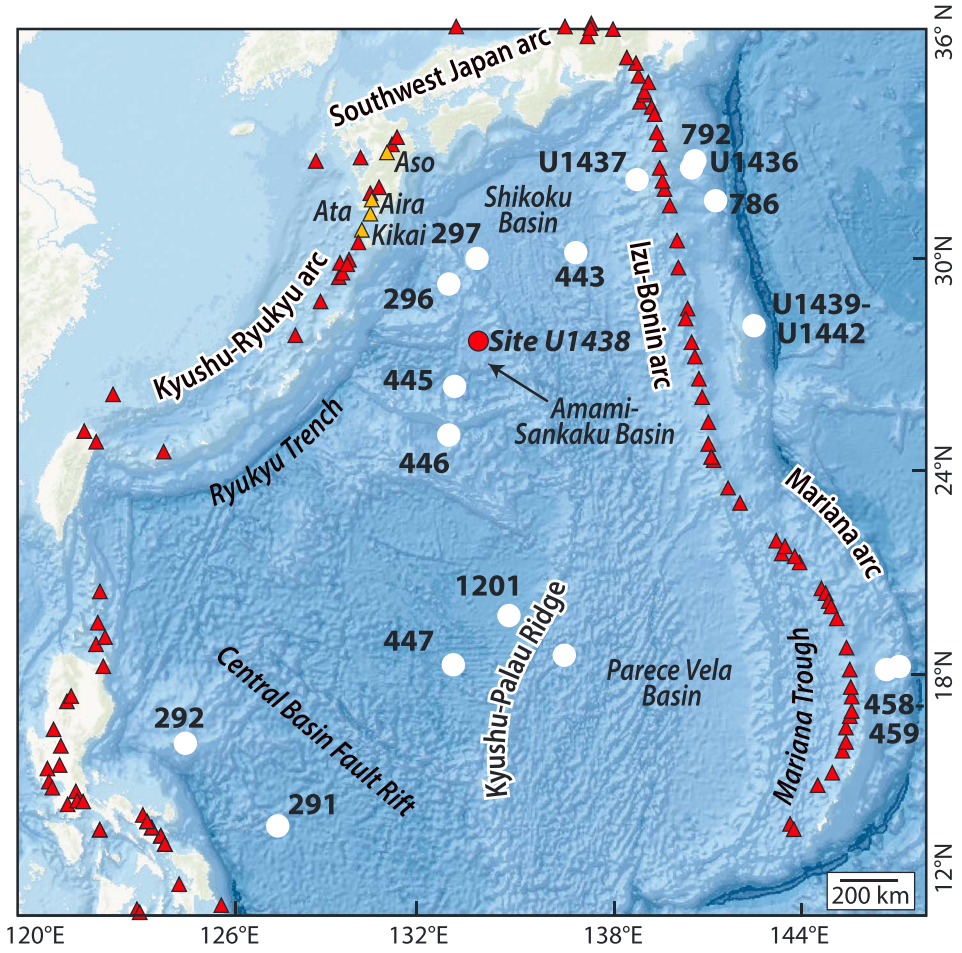

Figure 1. Map of the Western Pacific showing the West Philippine Basin, Izu-Bonin arc, and southwestern Japan. Red circle denotes the location of drill site U1438 drilled during IODP Expedition 351. White dots are locations of previous ocean drilling legs (Deep Sea Drilling Project, Ocean Drilling Program, and IODP) in the Western Pacific. Red triangles denote emergent volcanoes from the Smithsonian Global Volcanism database. IOD International Ocean Discovery program.

using high-resolution, color-scanned core images. Tephra layers were sampled onboard from IODP Holes U1438A and U1438B in Unit I (Arculus et al., 2015). The ashes form discrete layers (Figures 2a and 2b), often varicolored, 1–15 cm thick with most layers ranging from 1–4 cm in thickness and deposited between 0 and 4 Ma (Figures 3 and 4). The tephra usually show sharp to bioturbated basal contacts and gradational upper contacts into the mud, though both upper and lower contacts are often slightly to strongly bioturbated. One particular ash layer (Table 1) was found associated with a foraminiferal ooze, suggesting that the thickness might occasionally not be well constrained. Colorless vitric glass shards and pumices dominate the ash layers, with maximum grain sizes usually from 100–300 μm (Figures 2c–2f). The shards are angular and have well-preserved bubble walls (Figure 2c). Signs of alteration are rare and limited to the presence of spotted, whitish (less transparent) glass in certain samples (Table 1). Some tephra layers contain <1% pyroxene, amphibole, biotite ± zircon (e.g., Figure 2e). Representative unaltered tephra samples distributed throughout the last 4 Ma were sampled for Sr-Pb-Nd-Hf isotopes (Figure 4). Age-depth relationships for holes U1438A-B is based on the correlation between magnetozones and the geomagnetic polarity timescale (Arculus et al., 2015). The shipboard correlation of 87 geomagnetic reversals to the geomagnetic polarity timescale (Cande & Kent, 1995; Gradstein et al., 2012) at Site U1438 allows for high-resolution magnetostratigraphy up to Chron C16n.1r (36.051 Ma). For further details regarding the methods and correlations, the reader is referred to Arculus et al. (2015).

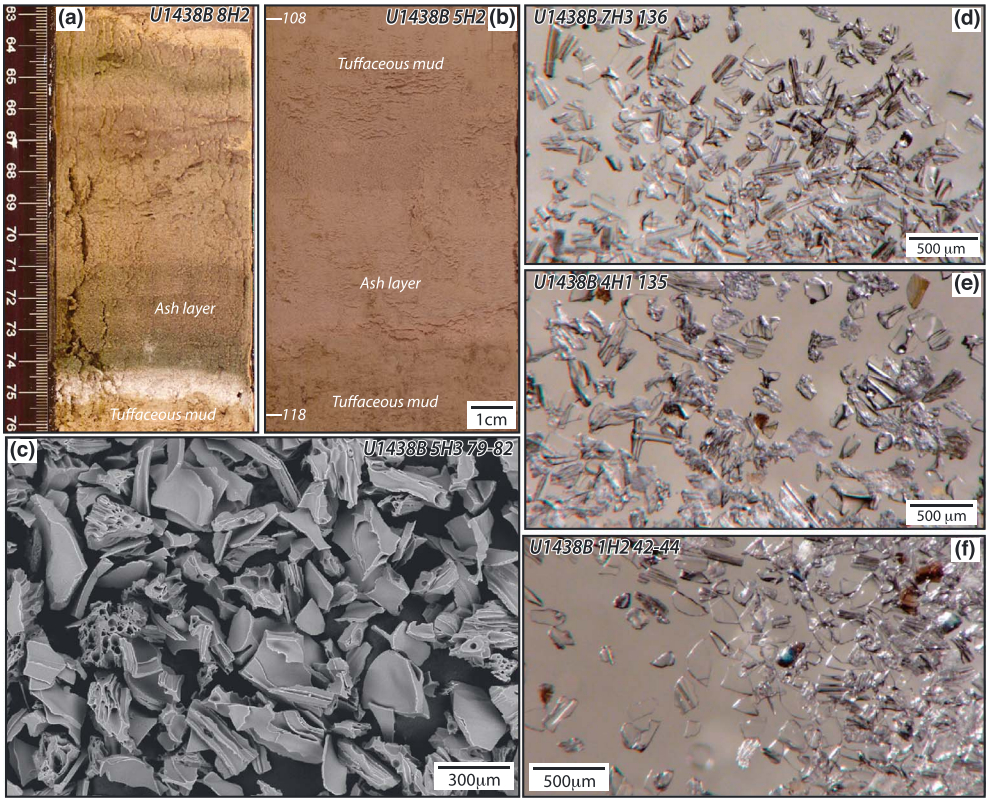

Figure 2. (a, b) Close-up images of U1438B cores of tuffaceous mud containing centimeter-thick ash layers; (c) scanning electron microscope image of cleaned ash shards; (d–f) close-up images of cleaned ash shards prepared for radiogenic isotope analysis. Note the clean, angular shape of glass shards and the local presence of magmatic minerals (amphibole in light brown).

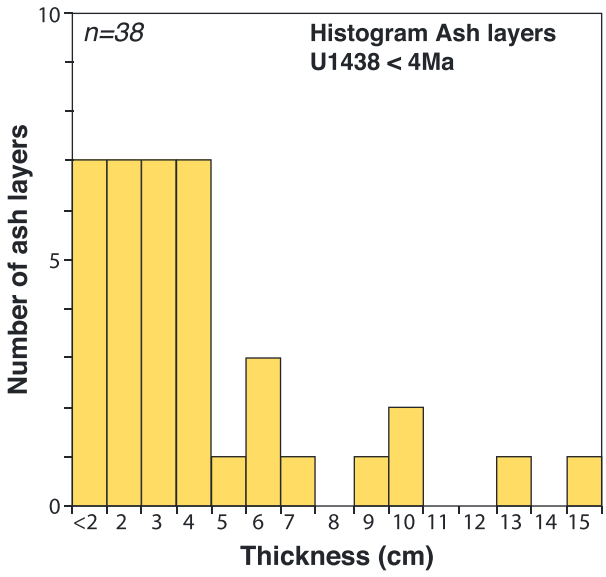

Figure 3. Thickness of ash layers younger than 4 Ma from IODP Site U1438 based on core descriptions of IODP Expedition 351 and scanned images of core sections. IODInternational Ocean Discovery program.

Samples were processed and analyzed at the School of Earth, Ocean, and Environment at the University of South Carolina (USA). Samples were wet-sieved between 180 and 90 µm using single-use Nylon sieves. In order to remove the clay fraction, 5 g/L of sodium hexametaphosphate Na-$(PO_3)_6$ was used to deflocculate the clay in an ultrasonic bath. This procedure was repeated until the water was clear. Rare carbonate was removed by letting samples rest in 15% HCl for up to 15 min. Samples were then repeatedly cleaned in 18 MΩ H_2O in order to remove any possible influence of Pb contamination from the Na-$(PO_3)_6$ (measured Pb contents of the Na-$(PO_3)_6$ were <0.45 ppb). Density separation by panning in order to remove the heavier mineral fraction was followed by hand picking underneath a microscope in order to produce 100–150 mg of pure glass shards (Figures 2d and 2e). Most samples are crystal poor or crystal free and dominated by colorless, transparent glass shards. Samples were then further rinsed three times in 18 MΩ H_2O prior to being digested for 24 hr in a 3:1 HF:HNO_3 mixture in capped Teflon vials. Digested samples were subsequently uncapped and dried down on a hot plate. Fluorides were removed by adding a 3–4 ml of concentrated HNO_3 followed by sealing the Teflon capsules at ~90 °C before being dried down again. This step was repeated three times.

After the final digestion steps, separate aliquots of the digest were processed for Nd, Sr, Pb, and Hf column chemistry. Rare earth elements were first isolated using the TRU-spec resin (Eichrom) in HNO_3. Neodymium

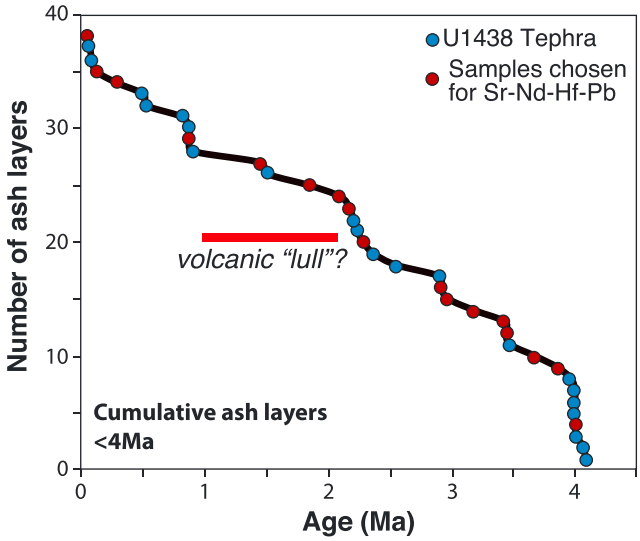

Figure 4. Cumulative number of ash layers within the last 4 Ma from Site U1438. Note that occasional hiatus occur, predominantly between 1 and 2 Ma. The lack of tephra between 1 and 2 Ma, suggesting a volcanic "lull," is consistent with less volcanism within Japan during that period (Mahony et al., 2016).

was then separated from this cut using LN-spec resin in HCl (e.g., Pin & Zalduegui, 1997). Hafnium was separated using a method modified after Münker et al. (2001). Pb was extracted in HNO_3-HBr extraction techniques in anion resin (e.g., Abouchami et al., 1999). Procedural blanks where always more than 1,000 lower than the amount of sample processed.

Isotope ratios were measured on the Thermo Finnigan Neptune Multi collector inductively coupled plasma source mass spectrometry (ICP-MS) at the Center for Elemental Mass Spectrometry at the University of South Carolina. Solutions were introduced with a 100-ml self-aspirating Teflon nebulizer (ESI, USA) coupled to an ESI APEX-Q system using a Jet sample cone and X-skimmer cone. Pb isotopes were measured using the Tl addition technique (White et al., 2000). Isotope ratios were corrected for fractionation using $^{203}Tl/^{205}Tl = 0.418911$ and the exponential law. Average ratios measured on NBS 981 standard solutions were $^{206}Pb/^{204}Pb = 16.9358 \pm 0.00097$, $^{207}Pb/^{204}Pb = 15.4893 \pm 0.00096$, and $^{208}Pb/^{204}Pb = 36.6927 \pm 0.0027$ (2 standard errors, $n = 13$). Sample compositions were corrected for instrumental bias using reference values for NBS 981 reported by Todt et al. (1996).

For Hf and Nd, the samples were diluted to achieve a signal of 2–5 V on ^{143}Nd and ^{176}Hf, and 30–45 analyses were run on each sample, depending on sample volume. Samples were bracketed every three to six solutions by the JNdi-1 standard for Nd, and the JMC-457 standard for Hf. Repeat analysis of U.S. Geological Survey rock standard AGV-1 ($n = 2$) run as an unknown agrees with published reference values of Weis et al. (2006, 2007) to within 0–0.4 epsilon units. The Hf and Nd isotopic composition of samples are reported relative to the accepted values for these standards ($^{176}Hf/^{177}Hf = 0.282160$; Vervoort & Blichert-Toft, 1999; $^{143}Nd/^{144}Nd=0.512115$, Tanaka et al., 2000).

Analyses of glass shards for major and minor elements were performed at Oregon State University with a CAMECA SX-100 electron microprobe using 15-keV accelerating voltage and 10-nA sample current. Counting times ranged from 10 to 60 s depending on the element and desired detection limit. In order to reduce the effects of alkali migration, the alkalis were measured first and a 0-time intercept function was applied to the data. Data reduction was performed online using a stoichiometric PAP correction model (Pouchou & Pichoir, 1984). All analyses are normalized to 100% to eliminate the effects of variable post depositional hydration. Analyses with total oxides less than 90 wt % were excluded from the data set. Laser ablation inductively coupled plasma mass spectrometer (LA-ICP-MS) analyses of trace elements in the same ash shards as microprobe analyses were performed using a Photon Machines Analyte G2 excimer laser system (ArF excimer 193 nm) coupled with a Thermo XSeries II quadrupole ICP-MS at the WM Keck Collaboratory for Plasma Spectrometry at Oregon State University. Shard analyses were conducted in spot mode using a masked spot rectangle of 27 μm × 75 μm, oriented along the long axis of the ash shard, with a laser pulse rate of 5 Hz, analysis time of ~45 s per spot, and laser energy fluence of 4.84 mJ/cm^2. Reference glass standard GSE-1G (analyzed after ~10 unknowns) was used for calibration, natural glass standards ATHO and BCR-2G (Jochum et al., 2005) as secondary standards to monitor accuracy and precision, and ^{29}Si was used as an internal standard in conjunction with SiO_2 contents measured by electron microprobe.

4. Results

Results are shown in Table 1 and plotted against age (depth) in Figure 6. The U1438 ashes show a narrow range in $^{87}Sr/^{86}Sr$ (0.704 to 0.706), $^{206}Pb/^{204}Pb$ (18.32 to 18.46), $^{207}Pb/^{204}Pb$ (15.57 to 15.62), and $^{208}Pb/^{204}Pb$ (38.46 to 38.75) with greater variation in ε_{Nd} (−3.5 to +4.8) and ε_{Hf} (+2.0 to +13.3). There is an inverse relationship between $^{87}Sr/^{86}Sr$ and $^{143}Nd/^{144}Nd$, with $^{87}Sr/^{86}Sr$ becoming gradually more radiogenic as $^{143}Nd/^{144}Nd$ becomes less radiogenic (Figure 7a). Major and trace element compositions indicate that all samples are rhyolitic, with >70 wt % SiO_2 and Na_2O+K_2O of 4–9 wt % (Figure 5 and the supporting

Table 1
Analyzed Rhyolite Tephra Samples (>99% Glass After Sample Cleaning and Sieving) and Measured Isotopic Compositions

Site/hole	U1438A	U1438A	U1438A	U1438B	U1438B	U1438B	U1438B	U1438B	U1438B
Core/Section	1H2W	1H4W	3H1W	1H2W	4H1W	4H6W	5H2W	5H3W	5H4W
Interval sampled (cm)	94–96	128–130	90–92	42–44	135–138	46–48	113–115	79–82	104–106
Thickness (cm)	2	10	2	2	9	3	4	3	1
Estimated Age (Ma)	0.12	0.28	0.91	0.04	1.45	1.84	2.10	2.17	2.28
minerals associated	—	—	biotite, amphibole	—	—	—	—	—	amphibole
Max shard size (μm)	300	350	300		200	200		100	300
glass alteration	unaltered	unaltered	unaltered	unaltered	unaltered, Found with Foraminifera ooze	slight devitrification of ash	unaltered	unaltered	slight devitrification of ash
Sm ppm	3.4	2.4	2.8	3.4	3.0	3.9	6.1	4.3	3.6
Nd ppm	15	15	16	18	15	20	26	22	14
$^{143}Nd/^{144}Nd$	0.512756	0.512582	0.512600	0.512461	0.512684	0.512793	0.512718	0.512770	0.512617
1σ	2	3	2	3	3	3	3	2	2
eNd_m	2.30	−1.09	−0.75	−3.45	0.89	3.03	1.55	2.57	−0.41
Rb ppm	87	97	109	124	106	106	76	88	119
Sr ppm	51	74	65	67	65	82	154	113	50
$^{87}Sr/^{86}Sr$	0.70471	0.70554	0.70505	0.70593	0.70533	0.70426	0.70449	0.70438	0.70578
1σ	1	1	1	1	1	1	1	1	1
$^{176}Hf/^{177}Hf$	0.283063	0.282927	0.282916	0.282830	0.283013	0.283116	0.283024	0.283094	0.282934
1σ	3	3	3	3	4	4	4	4	5
eHf_m	10.3	5.5	5.1	2.1	8.5	12.2	8.9	11.4	5.7
U ppm	2.3	1.8	2.5	2.5	2.9	2.6	1.6	1.9	2.3
Th ppm	8.2	11.2	9.8	12.1	11.4	11.5	12.5	12.0	10.1
Pb ppm	19.9	13.2	18.8	20.4	15.4	14.7	11.1	11.1	16.1
$^{206}Pb/^{204}Pb$	18.3877	18.4196	18.3588	18.3946	18.4056	18.4402	18.4397	18.4162	18.4630
1σ	3	2	3	2	2	3	2	2	3
$^{207}Pb/^{204}Pb$	15.569	15.600	15.585	15.598	15.598	15.594	15.599	15.592	15.620
1σ	3	2	3	2	2	3	2	2	3
$^{208}Pb/^{204}Pb$	38.459	38.619	38.555	38.631	38.647	38.646	38.660	38.623	38.747
1σ	1	1	1	1	1	1	1	1	1
Correlated with	Kikai Volcano (Kyushu)	Ryukyu Arc-Kyushu, ODP Leg 126 Hole 795 2H-2, 84-86	Ryukyu Arc-Kyushu: ODP Leg 126 Hole 811 8H-CC, 2-4	Aira-Tanzawa Volcano (Kyushu)	Ryukyu-Kyushu Arc	Ryukyu-Kyushu Arc	Ryukyu-Kyushu Arc	Ryukyu-Kyushu Arc	Ryukyu-Kyushu Arc

information). These compositions are similar to those of known rhyolitic caldera-forming eruptions over the last 5 Ma from throughout Japan (Kimura et al., 2015; Figure 5).

5. Discussion

5.1. The Source of Neogene and Quaternary Tephras From Site U1438

A depositional environment wherein fine-grained air-fall tephra are rapidly transported to the seafloor as gravity currents in the form of turbid plumes is likely (speeds >2 cm/s; e.g., Carey, 1997; Lowe, 2011). This implies that the tephra could have reached the floor of the ASB, currently at 4.8-km water depth, in ≤65 hr. Descending tephra plumes were therefore most likely not significantly affected by remobilization, redistribution by strong oceanic currents before final deposition at depth within the ASB. We conclude that the tephra are most likely to be distal air-fall deposits from explosive eruptions that occurred a few days prior to deposition. A rapid depositional environment and lack of remobilization of tephra layers is also consistent with the preserved angular shape of ash shards and the absence of identifiable seawater contamination (Figures 2 and 6b). Indeed, had seawater alteration affected the tephra compositions significantly, Sr isotopes would increase at constant ε_{Nd} due to the amount of radiogenic Sr in ocean water, as is shown in

Table 1
(continued)

Site/hole	U1438B	U1438B	U1438B	U1438B	U1438B	U1438B	U1438B	U1438B	U1438B
Core/Section	6H4W	6H5W	7H1W	7H3W	7H3W	7H5W	8H1W	8H2W	14H4W
Interval sampled (cm)	115–117	73–75	27.32	74–85	136–138	115–116	18–20	73–75	138–140
Thickness (cm)	2	15	10	8	4	2	6	1	3
Estimated Age (Ma)	2.91	2.98	3.19	3.43	3.47	3.67	3.86	4.00	14.67
minerals associated	amphibole	—	—	—	—	amphibole	plagioclase	—	biotite, amphibole, zircon
Max shard size (mm)	200	200	200	100	200				
glass alteration	unaltered	unaltered	unaltered	slight devitrification of ash	unaltered	slight devitrification of ash	unaltered	unaltered	unaltered
Sm ppm	3.0	4.3	2.9	3.1	6.7	2.9	4.3	6.1	2.4
Nd ppm	16	24	14	15	31	14	22	26	9
$^{143}Nd/^{144}Nd$	0.512721	0.512742	0.512681	0.512880	0.512677	0.512682	0.512649	0.512654	0.512555
1σ	3	3	3	3	2	2	2	3	3
eNd_m	1.62	2.03	0.84	4.73	0.76	0.86	0.21	0.31	−1.62
Rb ppm	102	99	103	51	102	99	124	102	189
Sr ppm	73	86	53	86	90	62	47	74	25
$^{87}Sr/^{86}Sr$	0.70455	0.70453	0.70535	0.70434	0.70497	0.70542	0.70586	0.70592	0.70735
1σ	1	1	1	1	1	1	1	1	1
$^{176}Hf/^{177}Hf$	0.282967	0.282979	0.282973	0.283149	0.282998	0.282989	0.282942	0.282958	0.282865
1σ	3	4	4	4	4	4	4	4	5
eHf_m	6.9	7.3	7.1	13.3	8.0	7.7	6.0	6.6	3.3
U ppm	2.4	2.1	2.1	1.2	2.2	2.1	2.2	1.9	4.1
Th ppm	11.7	14.7	11.2	5.5	12.1	9.2	14.4	10.5	7.4
Pb ppm	15.5	15.2	20.2	9.8	16.4	15.3	15.4	14.6	18.4
$^{206}Pb/^{204}Pb$	18.3303	18.3223	18.4735	18.3233	18.4276	18.4676	18.4483	18.4321	18.4354
1σ	3	2	3	2	2	3	2	3	2
$^{207}Pb/^{204}Pb$	15.575	15.571	15.615	15.577	15.601	15.618	15.617	15.612	15.598
1σ	3	2	3	2	2	3	2	3	2
$^{208}Pb/^{204}Pb$	38.485	38.465	38.712	38.477	38.632	38.740	38.725	38.706	38.650
1σ	1	1	1	1	1	1	1	1	1
Correlated with	Ryukyu-Kyushu Arc	Ryukyu-Kyushu Arc	Ryukyu-Kyushu Arc	Ryukyu-Kyushu Arc	Ryukyu-Kyushu Arc	Ryukyu-Kyushu Arc	Ryukyu-Kyushu Arc	Ryukyu-Kyushu Arc	Ryukyu-Kyushu Arc

the basement basalts from Site U1438 (e.g., Yogodzinski et al., 2018). Moreover, $^{87}Sr/^{86}Sr$ is not correlated with shard alteration (as indicated by patchy white, colorless glass). Thus, Sr isotopes appear to have been unaffected by interaction with seawater. In only one case (Table 1 and Figure 6b, tephra sample at age ca. 14 Ma) is it possible that $^{87}Sr/^{86}Sr$ might be affected by seawater alteration as neither Pb-Nd-Hf show any distinct composition shifts compared to other samples. Pb isotopes as well show no effect of alteration, as shown by their near homogenous $^{208}Pb/^{204}Pb$, $^{206}Pb/^{204}Pb$ and $^{207}Pb/^{204}Pb$ (Figure 6b), consistent with the lack of radiogenic Sr seawater alteration and the general elevated abundances of Pb in these tephra (10–20 ppm; Table 1 and the supporting information). Thus, Sr and Pb, reflect the magmatic isotopic composition of the tephra layers, as is the case for Hf and Nd isotopic ratios.

As can be seen in Figures 6–8, the isotopic and trace element ratios of the tephra from the ASB are distinct from IBM arc tephra. Figures 6a–6c and 7a and 7b show that the isotopic compositions of tephra and volcanic rocks from the IBM arc are more homogenous and clearly derived from more depleted sources than most volcanic samples from Northeast or Southwest Japan, or from the Kyushu-Ryukyu arc. This distinction has prevailed throughout the 50-Ma history of IBM Arc, which has produced volcanic rocks with ε_{Nd} of 5–10, $^{87}Sr/^{86}Sr$ <0.7045, and ε_{Hf} generally >14 (e.g.,Straub et al., 2015 ; Yogodzinski et al., 2018). In contrast, U1438 tephra have relatively unradiogenic Nd (ε_{Nd} +5 to −5) and Hf (ε_{Hf} +14 to +2) and relatively radiogenic Sr ($^{87}Sr/^{86}Sr$ >0.704). The fact that U1438 tephra are distinct from IBM volcanic rocks is further

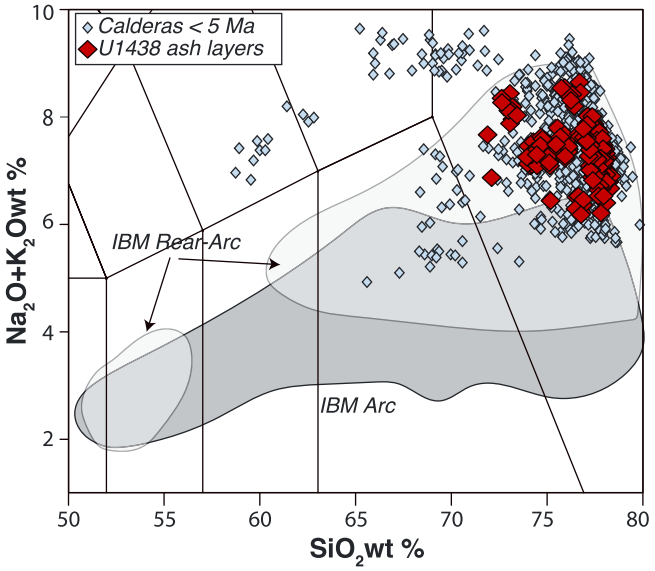

Figure 5. SiO_2wt % versus Na_2O + K_2O of U1438 ash layers compared to the Izu-Bonin Mariana (IBM) arc (Straub, 2003, and references therein) and calderas younger than 5 Ma (data from Kimura et al., 2015, Tsuji et al., 2017). Composition of glass shards can be found in the supporting information.

supported by the variation in ε_{Nd} with Sm/Nd (Figure 8). IBM arc rocks and tephra show a subhorizontal trend of decreasing Sm/Nd with nearly constant ε_{Nd}, which is controlled primarily by sedimentary inputs from the downgoing slab (Straub et al., 2015; Yogodzinski et al., 2018). In contrast rhyolitic tephra from the Kyushu-Ryukyu arc and silicic volcanism from the Honshu quaternary arc have lower Sm/Nd (<0.3) and ε_{Nd} (<5; Figures 6 and 8). In terms of Pb isotopes, U1438 tephra are homogenous and distinct from the array of volcanic rocks from the IBM arc (Figure 7), which have higher $^{208}Pb/^{204}Pb$ and $^{207}Pb/^{204}Pb$ for a given $^{206}Pb/^{204}Pb$ (Figures 6 and 7). The U1438 tephra are similar in this respect to rhyolitic tephra sampled from throughout Japan (Figure 7), though they have a significantly more restricted compositional variability. Thus, from first-order observations, it is clear that tephra younger than 4 Ma recovered from Site U1438 show no genetic relationship with the IBM Arc, but clear overlap isotopically with rhyolitic tephra from Honshu and Kyushu.

Kimura et al. (2015) assert that most rhyolitic tephra from the main Japanese Islands are formed through partial melting of the crust. This hypothesis is supported by the fact that the extended Pb isotopic range of the tephra mimics that of the crustal basement (Kimura et al., 2015). Alternatively, given the high abundances of Pb in crustal rocks compared to most mantle-derived rocks (e.g., Miller et al., 1994), it is possible that the Pb isotopic ratios of rhyolitic melts derived by fractional crystallization of more mafic parental magmas may be controlled by assimilation of a crustal component. The U1438 tephra only occupy a restricted portion of the Pb isotopic space defined by tephra from Japan (Figure 7). It is thus likely that the U1438 tephra originated from the islands of Honshu or Kyushu or from nearby islands that share a similar geologic history. Nevertheless, it is not possible to unambiguously distinguish sources in the Kyushu-Ryukyu, Southwestern, and Central Japan arcs using Pb isotopes alone (Kimura et al., 2015).

In terms of $^{87}Sr/^{86}Sr$ and ε_{Nd}, U1438 tephra overlap with isotopic compositions of known silicic eruptions from Kyushu, which overall show a limited range in $^{87}Sr/^{86}Sr$ (e.g., Ata, Aso, Aira, and Sendai ± Kirishima calderas, Arakawa et al., 1998; Figures 6g and 6h). Due to their generally more radiogenic Nd and less radiogenic Sr, U1438 tephra define a compositional array similar to silicic rocks from the Kyushu-Ryukyu arc, including samples from the Aso and Aira calderas (Figures 6g and 6h, 7a, and 8). On the same basis, the Site U1438 tephra appear unlike rhyolites and subvolcanic felsic plutons from Central Japan (Takedani Pluton, Hartung et al., 2017, and felsic volcanic eruptions, Kersting et al., 1996), which trend toward less radiogenic Nd and more radiogenic Sr (Figure 7). This is consistent with rhyolite melts having acquired part of their isotopic signature through interaction with Honshu basement crust, in part comprising isotopically distinct granites and gneisses that have highly radiogenic Sr, with $^{87}Sr/^{86}Sr$ ~0.7200, and unradiogenic Nd, with ε_{Nd} ~−15 (e.g., Arakawa & Shinmura, 1995). Moreover, the isotopic compositions of U1438 tephra show slightly higher $^{208}Pb/^{204}Pb$ and $^{207}Pb/^{204}Pb$ at a given $^{87}Sr/^{86}Sr$ than silicic Central Japan magmatism and overlap with silicic magmatism from the Ryukyu-Kyushu arc (Figures 7e and 7f). Thus, it is difficult to unambiguously distinguish specific possible source(s) for the U1438 tephra within Japan. Nonetheless, the homogenous Pb values and combined Sr-Nd isotopic data patterns are consistent with the hypothesis that these deposits were sourced from eruptions in a single region, most likely derived from within the Kyushu-Ryukyu arc.

In general, the distribution of tephra at Site U1438 (Figures 4 and 9) indicates a decrease in volcanic activity between 1 and 2 Ma, and more moderate volcanic activity between 2.8 and 3.5 Ma, with peak activity between 2 and 2.5 Ma, around 4 and circa <1 Ma. Based on the tephra record, volcanic activity observed in and around Japan over the last several Ma also shows periods of large-scale volcanism clustered around 4–6, 2–2.5, and <1 Ma (Mahony et al., 2016). Thus, the distribution in time of tephra at Site U1438 is broadly consistent with the known recent evolution of volcanism on the main islands of Japan. However, the Southwest Japan arc is an unlikely contributor to these rhyolite tephra, because it shows both a volcanic

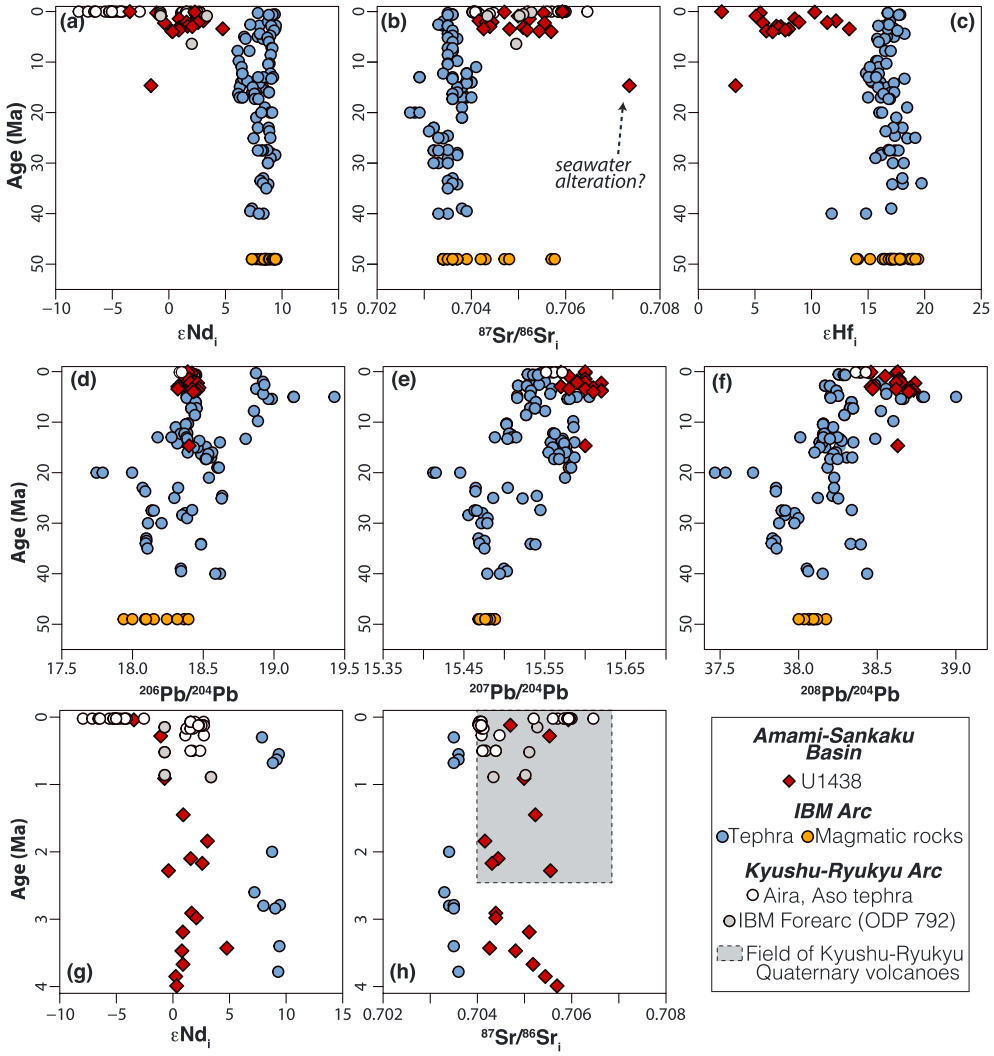

Figure 6. Radiogenic composition of U1438 ash layers as a function of age (depth) compared to the Izu-Bonin arc and representative caldera-forming eruptions from Kyushu (Aira and Aso volcanoes). (a–c) εNd_i, $^{87}Sr/^{86}Sr$ and εHf versus depth; (d–f) $^{206}Pb/^{204}Pb$, $^{207}Pb/^{204}Pb$, and $^{208}Pb/^{204}Pb$ with depth; (g and h) εNd_i, $^{87}Sr/^{86}Sr$ variations limited to the first 4 Ma only. Data for Aira Volcano from Arakawa et al. (1998). Data for Aso Volcano from Hunter (1998), Miyoshi et al. (2011), and Kaneko et al. (2015). IBM Arc tephra from Straub et al. (2004, 2009, 2010, 2015), Schmidt (2001), and Egeberg et al. (1992). ODP Site 792 in the IBM forearc shows preserved tephra suggested to derived from the Ryukyu arc (Egeberg et al., 1992). Field of Quaternary volcanoes (basalts to dacites) from Notsu et al. (1990). Magmatic rocks from the Izu-Bonin Arc are the underlying magmatic crust formed upon subduction initiation at 50 Ma (Yogodzinski et al., 2018). IBM = Izu-Bonin Mariana; ODOcean Drilling Program.

hiatus between 5 and 3 Ma and a lack of caldera-forming eruptions from 3–0 Ma (Kimura et al., 2005, 2014; Figure 9). Volcanism in Central Japan (Norikura segment) shows an increase in activity between 1.8 and 2.5 Ma (Kimura et al., 2015; Mahony et al., 2016) and could thus be contributing to the U1438 tephra at 2–2.5 Ma (Figure 9), but the generally less radiogenic $^{87}Sr/^{86}Sr$ and more radiogenic ε_{Nd} of Site U1438 rhyolites makes this unlikely. On the other hand, there are a number of observations consistent with an origin for U1438 within the Kyushu-Ryukyu arc. These are (1) the observed increase in magmatism ranging from basalt to rhyolite in the Central Ryukyu arc at circa 4–6 Ma (Shinjo et al., 1999 and references therein); (2) the occurrence of contemporaneous and large caldera-forming eruptions in Central Kyushu (e.g., the 1.3- to 0.6-Ma ignimbrites) and in Southern Kyushu (Kagoshima volcanotectonic graben) including the Kikai, Ata, and Aira calderas (Shinjo et al., 2000; Figure 7); and (3) the overlap of isotopic signatures of U1438 and Kyushu-Ryukyu rhyolites, combined with a lack of significant isotopic heterogeneity in U1438 rhyolites over the last 4 Ma (Figures 6 and 7).

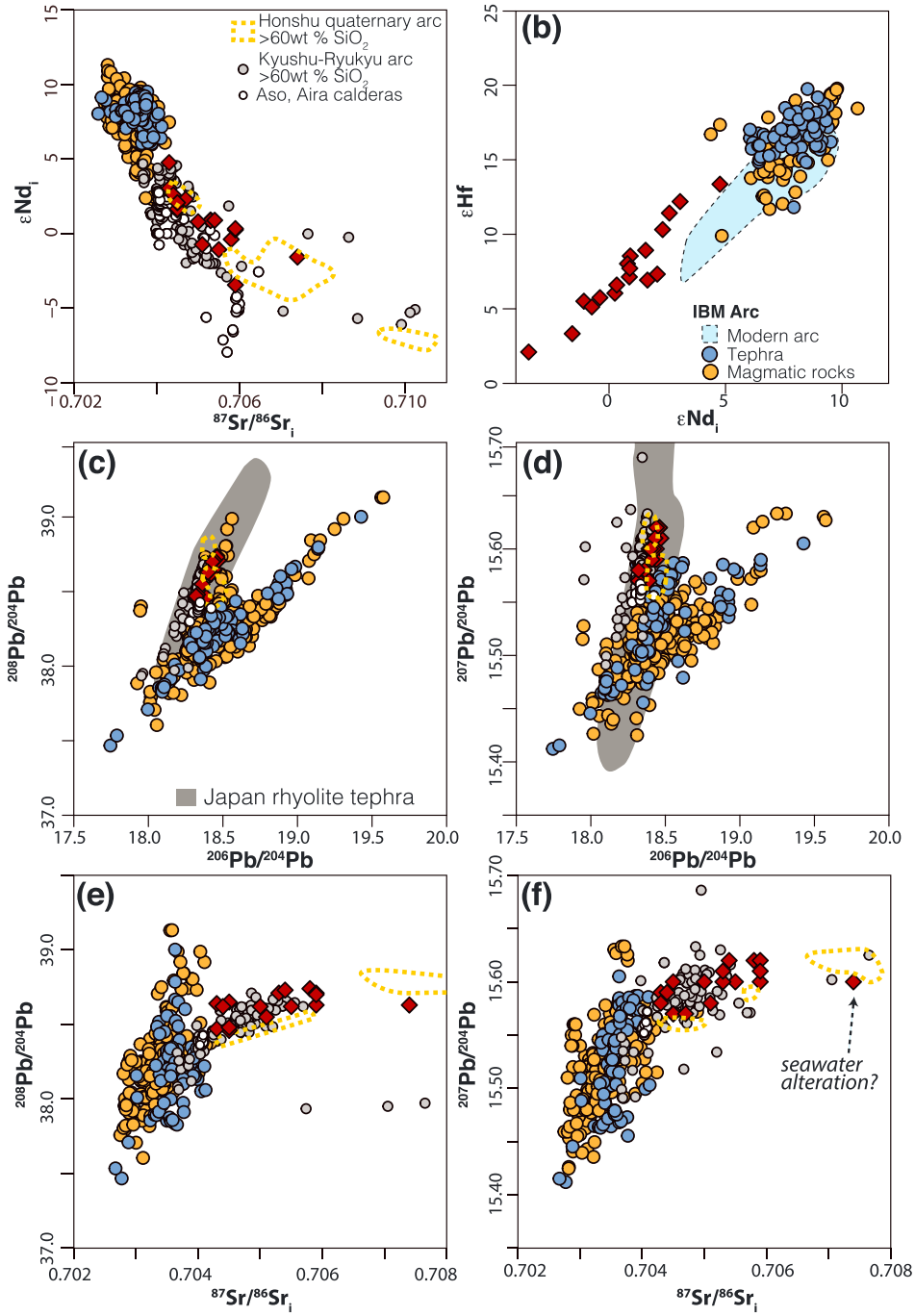

Figure 7. Radiogenic isotope composition of U1438 ash layers: (a) εNd_i versus $^{87}Sr/^{86}Sr_i$; (b) εHf versus εNd_i; (c) $^{208}Pb/^{204}Pb$ versus $^{206}Pb/^{204}Pb$; (d) $^{207}Pb/^{204}Pb$ versus $^{206}Pb/^{204}Pb$; (e) $^{208}Pb/^{204}Pb$ versus $^{87}Sr/^{86}Sr$, and (f) $^{207}Pb/^{204}Pb$ versus $^{87}Sr/^{86}Sr$. The yellow field of Honshu quaternary arc volcanoes includes quaternary rhyolites and the Takidani granodiorites and is from Kersting et al. (1996), Kimura and Nagahashi (2007), Kersting et al. (1996), and Hartung et al. (2017). Note that in (a), quaternary Honshu rhyolites have values reaching $\varepsilon Nd = -6.75$ and $^{87}Sr/^{86}Sr = 0.70956$ (Nikko Shirani Volcano; Kersting et al., 1996). Basement rocks from Honshu reach $\varepsilon Nd = -15.6$ and $^{87}Sr/^{86}Sr$ of 0.7200 (Arakawa & Shinmura, 1995). Pb isotopes for Honshu quaternary arc are from the Takadani Pluton (Hartung et al., 2017) and the Chayano-Ebisutoge Rhyolite (Kimura & Nagahashi, 2007). Kyushu and Ryukyu volcanic rocks from Terakado et al. (1988), Shinjo (1998), Shinjo et al. (1999, 2000), Arakawa et al. (1998), Furukawa et al. (2009), Guo et al. (2016), Hoang and Uto (2006), Honma et al. (1991), Hosono et al. (2008), Hunter (1998), Kaneko et al. (2015), Kita et al. (2012), Miyoshi et al. (2011), and Shibata et al. (2013, 2014). For the Izu-Bonin Mariana field (uncorrected for time) a compilation of magmatic products from arc-inception (ca. 50 Ma) to quaternary magmatic products are included: Yogodzinski et al. (2018), Reagan et al. (2010) (subduction-initiation magmatism at ca. 50 Ma; Ishizuka et al. (2011; Kyushu-Palau Ridge), Ishizuka et al. (2006, 2007, 2009), Hochstaedter et al. (2001), Kuritani et al. (2003), Tollstrup et al. (2010), Taylor and Nesbitt (1998), Pearce et al. (1992, 1999), Woodhead (1989), and White and Patchett (1984). IBM = Izu-Bonin Mariana.

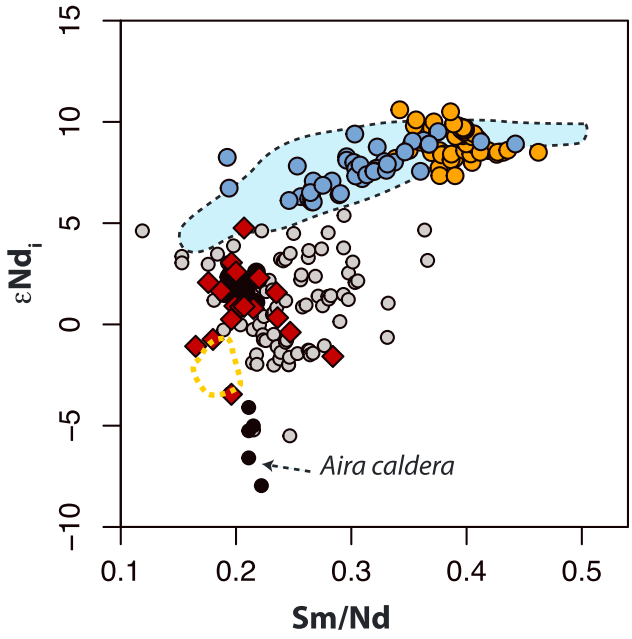

Figure 8. Neodymium isotopes (εNd) versus Sm/Nd, comparing tephra, igneous basement and modern volcanic rocks from the Izu-Bonin Arc with volcanic rocks and tephra from the Ryukyu arc, Shikoku and Honshu. Tephra from Site U1438 shows distinct compositions consistent with provenance from the southwestern Japan and the Kyushu-Ryukyu arc. Field for the modern IBM arc after Yogodzinski et al. (2018). Note that the Sm/Nd ratio of melt inclusions in volcaniclastic sediments from U1438 (25 to 50 Ma) range from 0.17 to 0.51, overlapping the range of the Izu-Bonin Mariana arc (Brandl et al., 2017).

In Japan, most late Quaternary tephra are distributed to the east of their source volcanoes, because the plumes are transported by the prevailing westerly winds (Machida & Arai, 2003). It is thus unsurprising that the isotopic record of rhyolitic tephra at Site U1438 is consistent with sources in the Kyushu-Ryukyu arc. As the demise of volcanic activity at the KPR at ~25 Ma (Ishizuka et al., 2011) was subsequently followed by subduction initiation along the Kyushu-Ryukyu arc at 15 Ma (Wu et al., 2016), it is likely that the approach of Site U1438 to the Ryukyu-Kyushu arc led to an increase in the frequency of ash deposition at the site.

5.2. Correlating Individual Tephra Layers Within the Kyushu-Ryukyu Arc

Our ability to correlate individual ash layers with known volcanic sources is hampered by the lack of detailed isotopic data for tephra throughout Japan and by the overall lack of well-constrained rhyolitic tephra deposited in SW Japan since ~1 Ma (Kimura et al., 2015). Machida (1999, 2002) and Kimura et al. (2015) correlated 15 tephra layers from the Kyushu-Ryukyu arc in the last 1 Ma with well-known tephra markers throughout Japan (Figure 9), but major tephra markers in SW Japan in the 1- to 4-Ma time window remain scarce. There have been several caldera-forming eruptions Quaternary in the Kyushu-Ryukyu Arc, including those at Aso, Aira, Ata, Kikai, Kakuto-Kobayashi, and Shishimita (e.g., Arakawa et al., 1998; Machida & Arai, 2003), but most tephras from these eruptions do not appear to be well preserved at Site U1438. The great distance from the source could be the main reason for the patchy record of certain caldera-forming silicic eruptions from Kyushu, as Site U1438 is close to the distal limits of known tephra fallout of certain caldera-forming eruptions (Machida, 1999; Machida & Arai, 2003; Tsuji et al., 2017). It is also possible that the water depth at Site U1438 might induce localized heterogeneous distribution of tephra on the seafloor during deposition by density currents. As shown in Allan et al. (2008), tephra preservation can be patchy at a given drill site, with individual cores only sampling a limited proportion of tephra layers deposited in across a basin. Thus, the lack of evidence of certain large-scale Quaternary eruptions is unsurprising. Nevertheless, based on Sr-Nd isotopic composition, depositional age, and overlapping major element compositions of ash shards compared to tephra samples of known rhyolitic eruptions measured by Tsuji et al. (2017) and Kimura et al. (2015), we are confident that the caldera-forming eruption of Aira (*Aira-Tanzawa Tephra, AT*), the most prominent tephra marker in the late Pleistocene at circa 29 ka (Machida et al., 2002), and Kikai Volcano (*eruption at 77–101 ka, K-Tz*; Machida & Arai, 1992, Tatsumi et al., 2018) are well preserved within the tephra record of U1438 (Table 1). The 2-cm-thick ash falls from the *Aira* and *Kikai* eruptions are also consistent with the estimated thickness of tephra deposits at this location according to tephra isopach maps of Machida (1999).

Figures 6g and 6h and 9 show that the depositional age and isotopic composition of several tephra layers from the IBM forearc and sampled during ODP Leg 792 (Egeberg et al., 1992) are similar to those at Site U1438. This supports the interpretation proposed by Egeberg et al. (1992) and more recently by Kutterolf et al. (2018) and Schindlbeck et al. (2018) that occasional tephra markers within the IBM arc (Figure 1 for location of ODP Site 792, IODP Exp. 350 Sites U1436-U1437 and IODP Exp. 352 Sites U1439-U1442) are derived from the Kyushu-Ryukyu arc. Occurrence of AT tephra and Kikai-Akahoya (K-Ah) tephra on some Izu-Bonin islands (e.g., Ishizuka & Geshi, 2018) provides further support for this interpretation. Additional correlations for tephra at 2–4 Ma might be possible on the basis of the 2- to 4-Ma tuff layers (rhyolites) in the Miyazaki Group from the Miyazaki basin in the southeastern part of Kyushu (Torii et al., 2000; Figure 9), but the lack of isotopic data and imprecise age estimates for the subaerial deposits means that such correlations would be tenuous.

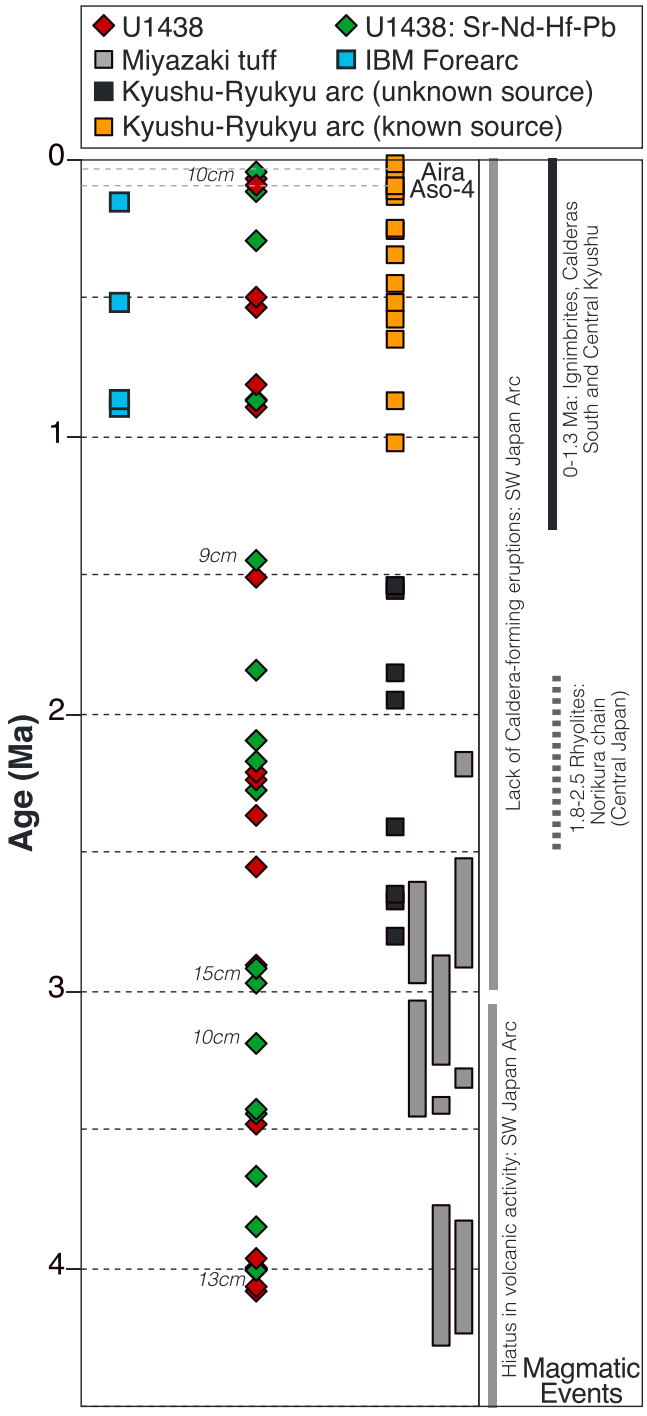

Figure 9. Plot showing the age of known and unknown tephra derived from the Ryukyu-Kyuhsu arc compared to the age of U1438 tephra. The thickness of thick U1438 tephra is shown in italic next to the layer. Ash layers for Kyushu from Machida (1999, 2002), Kimura et al. (2015, and references therein), Torii et al. (2000), and Torii and Oda (2001). Note the relatively large errors of the Myazaki tuff (Torii et al., 2000). Timing of South and Central Kyushu ignimbrites after Kamata and Kodama (1999, and references therein) and Kimura et al. (2015). ODP Leg 792 in the Izu-Bonin Mariana forearc shows preserved tephra suggested to derive from the Ryukyu arc (Egeberg et al., 1992). Hiatus in volcanism after Kimura et al. (2005, 2014). Central Japan data after Kimura et al. (2015).

We find that the predominant source(s) of the U1438 rhyolitic tephra lie predominantly within the Kyushu-Ryukyu arc, but the exact volcanic source(s) of most of the layers remain unknown. The abundance of caldera-forming eruptions from the Kyushu-Ryukyu arc, which dominate the sedimentary deposits of ocean basins to the east of their location, as shown by the abundance of rhyolitic tephra from Kyushu-Ryukyu arc in the ASB and not from the IBM arc, is also consistent with recent studies showing that tephra from the Kyushu-Ryukyu arc and Central Japan arc contribute significantly to the sedimentary record within the IBM system (Egeberg et al., 1992; Kutterolf et al., 2018; Schindlbeck et al., 2018) and broader Pacific region (e.g., Scudder et al., 2016).

5.3. Implications for Large Rhyolitic Eruptions in Southwest Japan at 0–4 Ma

Though Site U1438 is located at the closest, ~50 km from the KPR, the isotopic composition of the tephra imply a source within the Kyushu-Ryukyu arc. At present, Site U1438 is located ~600 km from Central Ryukyu (*Io-Torishima Volcano*), 590 km from South Kyushu (*Aira Volcano)* and 680 km from Central Kyushu (*Aso Volcano*). Site U1438 is significantly farther away from Southwest Japan than other drill sites with important tephra records on the Philippine Sea plate, such as Deep Sea Drilling Project sites 296 and 297 (e.g., Ingle et al., 1975), both of which are 300–400 km from Central Kyushu calderas. As Site U1438 is located on the Philippine Sea plate, the location of the drill site became closer to Southwest Japan with time. Assuming a subduction rate at the Kyushu-Ryukyu Trench of ~ 6 cm/year, the site could have been ~240 km further to the southeast from its current location at 4 Ma. The tephra layers would therefore have been derived from eruptive centers located at distances of greater than 800 km. Though preservation of thick tephra deposits in ocean sediments is not unusual, as shown in the IBM forearc and in the Shikoku and Ryukyu sedimentary basins (e.g., Egeberg et al., 1992; Reagan et al., 2015; Straub et al., 2015; Tsuji et al., 2017), preservation of thick tephra layers from eruptive centers situated at such distances (>600 km) are significantly less common (e.g., Schindlbeck et al., 2018). Mahony et al. (2016) modeled the tephra thickness with distance to the volcanic source as a function of eruption magnitude, demonstrating that tephra deposited several hundreds of kilometers from the trench are most likely to be related to large (>M5) caldera-forming eruptions. Moreover, Schindlbeck et al. (2018) estimated the magnitude of volcanic eruptions based on tephra thickness recovered at IODP Site U1437 within the IBM forearc, and distance from a known source in Kyushu, as M6.3–7.3. We conclude the thick ash layers at Site U1438, allowing for the age-distance relations from the Kyushu-Ryukyu arc, record >M6 eruptions. Though such large-scale eruptions should be identifiable by the presence of widespread tephra deposits in and around Japan and the Philippine Sea, there is, as of now, no clear silicic tephra record of volcanic eruption from the Kyushu-Ryukyu arc that can be clearly linked to thicker tephra fallout at circa 1.5, 3.0–3.2, and 4.1 Ma (Kimura et al., 2015; Machida, 2002; Figure 9). We suggest that the location of the deep (4.8-km water depth) ASB located >600km from the Kyushu-Ryukyu arc makes it an ideal candidate to identify currently unknown large-scale eruptions that occurred in the Neogene and Quaternary. High-precision dating and isotope analysis of such calderas and sedimentary basins containing an array of tephra markers (e.g., Miyazaki Basin) could help constrain the history of explosive eruptions

in southwestern Japan, with Site U1438 in the ASB representing a crucial marker of large, caldera-forming rhyolitic eruptions in the last 4 Ma within the Kyushu-Ryukyu arc. We suggest that unidentified, submerged large-scale calderas within the Kyushu-Ryukyu arc, similar to submerged calderas already known to exist within the northern IBM arc (e.g., *Sumisu caldera*, Tani et al., 2008) and Northern Ryukyu (*Shishimuta Caldera*, Kamata, 1989) might in part be responsible from these tephra deposits, as well as unidentified older historical eruptions from known calderas within Kyushu.

6. Conclusions

Isotopic analysis of ash layers from IODP Expedition 351 indicates the tephra layers at Site U1438 from the ASB preserve a record of rhyolitic eruptions derived primarily from the Kyushu-Ryukyu arc, with no clear evidence of any significant eruptions derived from Central Honshu, southwestern Japan,and the IBM arc. The tephra record at Site U1438 can in part be correlated with Quaternary eruptions of Aira and Kikai on Kyushu Island, though other crucial markers seem to be missing. The <4-Ma tephra record from IODP Site U1438 records significant tephra accumulations (9–15 cm thick) from rhyolitic eruptions for which volcanic source(s) are as yet unconstrained but were at considerable distance from Site U1438 (>600 km). The implication is that the eruptions must have been M > 6. The unique rhyolitic tephra record of Site U1438 might therefore be used as a marker for caldera-forming eruptions within the Kyushu-Ryukyu arc over the last 4 Ma.

Acknowledgments

A. M. acknowledges support from the Swiss National Science Foundation (grant 200020/135511 to Othmar Müntener and grant P2LAP2_171819 to A. M.) and Swiss IODP. This work was also supported by grants to G. M. Y. and M. B. from NSF (OCE-1537135) and IODP. The authors thank W. Buckley at the Center for Elemental Mass Spectrometry for their assistance with data collection at the University of South Carolina. The work and assistance of the captain and crew of the R/V JOIDES Resolution are gratefully acknowledged. We are grateful for reviews by J. Schindlbeck and S. Kutterolf as well as editorial handling by M. Edmonds. The full description of Site U1438 cores can be accessed publicly from http://web.iodp.tamu.edu/LORE/ website. Geochemical analyses of glass shards are accessible in the supporting information data set.

References

Abouchami, W., Galer, S. J. G., & Koschinsky, A. (1999). Pb and Nd iotopes in NE Atlantic Fe-Mn crusts: proxies for trace metal plaeosources and paleocean circulation. *Geochimica et Cosmochimica Acta*, *63*(10), 1489–1505. https://doi.org/10.1016/S0016-7037(99)00068-X

Allan, A. S., Baker, J. A., Carter, L., & Wysozanski, R. J. (2008). Reconstructing the Quaternary evolution of the worlds most active silicic volcanic systems: insights from an 1.65 Ma deep ocean tephra record sourced from Taupo Volcanic Zone, New Zealand. *Quaternary Science Reviews*, *27*(25-26), 2341–2360. https://doi.org/10.1016/j.quascirev.2008.08.003

Arakawa, Y., Kurosawa, M., Takahashi, K., Kobayashi, Y., Tsukui, M., & Amakawa, H. (1998). Sr–Nd isotopic and chemical characteristics of the silicic magma reservoir of the Aira pyroclastic eruption, southern Kyushu, Japan. *Journal of Volcanology and Geothermal Research*, *80*(3-4), 179–194. https://doi.org/10.1016/S0377-0273(97)00046-2

Arakawa, Y., & Shinmura, T. (1995). Nd-Sr isotopic and geochemical characteristics of two contrasting types of calc-alkaline plutons in the Hida belt, Japan. *Chemical Geology*, *124*(3-4), 217–232. https://doi.org/10.1016/0009-2541(95)00012-B

Arculus, R. J., Ishizuka, O., Bogus, K., Aljahdali, M. H., Bandini-Maeder, A. N., Barth, A. P., et al. (2015). Site U1438. In R. J., Arculus, O. Ishizuka, K., Bogus, and the Expedition 351 Scientists (Eds.), *Proceedings of the International Ocean Discovery Program, Expedition 351:Izu-Bonin-Mariana Arc Origins*. College Station, TX: International Ocean Discovery Program. https://doi.org/10.14379/iodp.proc.351.103.2015

Brandl, P. A., Hamada, M., Arculus, R. J., Johnson, K., Marsaglia, K. M., Savov, I. P., et al. (2017). The arc arises: The links between volcanic output, arc evolution and melt composition. *Earth and Planetary Science Letters*, *461*, 73–84. https://doi.org/10.1016/j.epsl.2016.12.027

Cande, S. C., & Kent, D. V. (1995). Revised calibration of the geomagnetic polarity timescale for the Late Cretaceous and Cenozoic. *Journal of Geophysical Research*, *100*(B4), 6093–6095. https://doi.org/10.1029/94JB03098

Carey, S. (1997). Influence of convective sedimentation on the formation of widespread tephra fall layers in the deep sea. *Geology*, *25*(9), 839–842. https://doi.org/10.1130/0091-7613(1997)025<0839:IOCSOT>2.3.CO;2

DeCelles, P. G., Ducea, M. N., Kapp, P., & Zandt, G. (2009). Cyclicity in Cordilleran orogenic systems. *Nature Geoscience*, *2*(4), 251–257. https://doi.org/10.1038/ngeo469

Ducea, M. N., Saleeby, J. B., & Bergantz, G. (2015). The architecture, chemistry, and evolution of continental magmatic arcs. *Annual Review of Earth and Planetary Sciences*, *43*(1), 299–331. https://doi.org/10.1146/annurev-earth-060614-105049

Egeberg, P. K., Brunfelt, A. O., & Stabel, A. S. (1992). Characterization and correlation of megascopic tephras in Site 792 cores from the Izu-Ogasawara forearc basin (Japan) by trace elements and 87Sr/86Sr and 143Nd/144Nd isotopes. *Proceeding of the Ocean Drilling Program, Scientific Results*, *126*, 457–465. https://doi.org/10.2973/odp.proc.sr.126.149.1992

Furukawa, K., Miyoshi, M., Shinmura, T., Shibata, T., & Arakawa, Y. (2009). Geology and petrology of the Pre-Aso volcanic rocks distributed in the NW wall of Aso caldera: Eruption style and magma plumbing system of the pre-caldera volcanism. *Journal of Geological Society of Japan*, *115*(12), 658–671. https://doi.org/10.5575/geosoc.115.658

Gradstein, F. M., Ogg, J. G., Schmitz, M. D., & Ogg, G. M. (Eds) (2012). *The geological time scale*. Amsterdam: Elsevier.

Guo, K., Zhai, S., Yu, Z., Wang, S., Zhang, X., & Wang, X. (2016). Geochemical and Sr-Nd-Pb-Li isotopic characteristics of volcanic rocks from the Okinawa Trough: Implications for the influence of subduction components and the contamination of crustal materials. *Journal of Marine Systems*, *180*, 140–151. https://doi.org/10.1016/j.jmarsys.2016.11.009

Hartung, E., Caricchi, L., Floess, D., Wallis, S., Harayama, S., Kouzmanov, K., & Chiaradia, M. (2017). Evidence for residual melt extraction in the Takidani Pluton, Central Japan. *Journal of Petrology*, *58*(4), 763–788. https://doi.org/10.1093/petrology/egx033

Hoang, N., & Uto, K. (2006). Upper mantle isotopic components beneath the Ryukyu arc system: Evidence for 'back-arc'entrapment of Pacific MORB mantle. *Earth and Planetary Science Letters*, *249*(3), 229–240. https://doi.org/10.1016/j.epsl.2006.07.021

Hochstaedter, A., Gill, J., Peters, R., Broughton, P., Holden, P., & Taylor, B. (2001). Across-arc geochemical trends in the Izu-Bonin arc: Contributions from the subducting slab. *Geochemistry, Geophysics, Geosystems*, *2*(7). https://doi.org/10.1029/2000GC000105

Honma, H., Kusakabe, M., Kagami, H., Iizumi, S., Sakai, H., Kodama, Y., & Kimura, M. (1991). Major and trace element chemistry and D/H, 18O/16O, 87Sr/86Sr and 143Nd/144Nd ratios of rocks from the spreading center of the Okinawa Trough, a marginal back-arc basin. *Geochemical Journal*, *25*(2), 121–136. https://doi.org/10.2343/geochemj.25.121

Hosono, T., Nakano, T., Shin, K., & Murakami, H. (2008). Assimilation of lower to middle crust by high alumina basalt magma as an explanation for the origin of medium-K volcanic rocks in southern Kyushu, Japan. *Lithos*, *105*(1), 51–62. https://doi.org/10.1016/j.lithos.2008.02.007

Hunter, A. G. (1998). Intracrustal controls on the coexistence of tholeiitic and calc-alkaline magma series at Aso volcano, SW Japan. *Journal of Petrology*, *39*(7), 1255–1284. https://doi.org/10.1093/petroj/39.7.1255

Ingle, J. C., Karig, D. E., White, S. M., & Shipboard Scientific Party (1975). DSDP Volume 31. In D. E. Karig, J. C. Ingle, & Shipboard Scientific Party (Eds.), *Initial Reports of the Deep Sea Drilling Project*, (Vol. 31, pp. 5–21). Washington, DC: U.S. Government Printing Office.

Ishizuka, O., and Geshi, N., (2018), Geological map of Hachijojima Volcano. Geological map of volcanoes, No. 20, Geological Survey of Japan, AIST.

Ishizuka, O., Hickey-Vargas, R., Arculus, R. J., Yogodzinski, G. M., Savov, I. P., Kusano, Y., et al. (2018). Age of Izu–Bonin–Mariana arc basement. *Earth and Planetary Science Letters*, *481*, 80–90. https://doi.org/10.1016/j.epsl.2017.10.023

Ishizuka, O., Kimura, J. I., Li, Y. B., Stern, R. J., Reagan, M. K., Taylor, R. N., et al. (2006). Early stages in the evolution of Izu–Bonin arc volcanism: New age, chemical, and isotopic constraints. *Earth and Planetary Science Letters*, *250*(1), 385–401. https://doi.org/10.1016/j.epsl.2006.08.007

Ishizuka, O., Taylor, R. N., Yuasa, M., Milton, J. A., Nesbitt, R. W., Uto, K., & Sakamoto, I. (2007). Processes controlling along-arc isotopic variation of the southern Izu-Bonin arc. *Geochemistry, Geophysics, Geosystems*, *8*, Q06008. https://doi.org/10.1029/2006GC001475

Ishizuka, O., Taylor, R. N., Yuasa, M., & Ohara, Y. (2011). Making and breaking an island arc: A new perspective from the Oligocene Kyushu-Palau arc, Philippine Sea. *Geochemistry, Geophysics, Geosystems*, *12*, Q05005. https://doi.org/10.1029/2010GC003440

Ishizuka, O., Yuasa, M., Taylor, R. N., & Sakamoto, I. (2009). Two contrasting magmatic types coexist after the cessation of back-arc spreading. *Chemical Geology*, *266*(3), 274–296. https://doi.org/10.1016/j.chemgeo.2009.06.014

Jochum, K. P., Willbold, M., Raczek, I., Stoll, B., & Herwig, K. (2005). Chemical Characterisation of the USGS Reference Glasses GSA-1G, GSC-1G, GSD-1G, GSE-1G, BCR-2G, BHVO-2G and BIR-1G Using EPMA, ID-TIMS, ID-ICP-MS and LA-ICP-MS. *Geostandards and Geoanalytical Research*, *29*(3), 285–302. https://doi.org/10.1111/j.1751-908X.2005.tb00901.x

Kamata, H. (1989). Shishimuta caldera, the buried source of the Yabakei pyroclastic flow in the Hohi volcanic zone, Japan. *Bulletin of Volcanology*, *51*(1), 41–50. https://doi.org/10.1007/BF01086760

Kamata, H., & Kodama, K. (1999). Volcanic history and tectonics of the Southwest Japan Arc. *Island Arc*, *8*(3), 393–403. https://doi.org/10.1046/j.1440-1738.1999.00241.x

Kaneko, K., Inoue, K., Koyaguchi, T., Yoshikawa, M., Shibata, T., Takahashi, T., & Furukawa, K. (2015). Magma plumbing system of the Aso-3 large pyroclastic eruption cycle at Aso volcano, Southwest Japan: Petrological constraint on the formation of a compositionally stratified magma chamber. *Journal of Volcanology and Geothermal Research*, *303*, 41–58. https://doi.org/10.1016/j.jvolgeores.2015.07.016

Kersting, A. B., Arculus, R. J., & Gust, D. A. (1996). Lithospheric contributions to arc magmatism: isotope variations along strike in volcanoes of Honshu, Japan. *Science*, *272*(5267), 1464–1468.

Kimura, J. I., Gill, J. B., Kunikiyo, T., Osaka, I., Shimoshioiri, Y., Katakuse, M., et al. (2014). Diverse magmatic effects of subducting a hot slab in SW Japan: Results from forward modeling. *Geochemistry, Geophysics, Geosystems*, *15*, 691–739. https://doi.org/10.1002/2013GC005132

Kimura, J. I., & Nagahashi, Y. (2007). Origin of a voluminous iron-enriched high-K rhyolite magma erupted in the North Japan Alps at 1.75 Ma: Evidence for upper crustal melting. *Journal of Volcanology and Geothermal Research*, *167*(1), 81–99. https://doi.org/10.1016/j.jvolgeores.2007.02.004

Kimura, J. I., Nagahashi, Y., Satoguchi, Y., & Chang, Q. (2015). Origins of felsic magmas in Japanese subduction zone: Geochemical characterizations of tephra from caldera-forming eruptions< 5 Ma. *Geochemistry, Geophysics, Geosystems*, *16*, 2147–2174. https://doi.org/10.1002/2015GC005854

Kimura, J. I., Stern, R. J., & Yoshida, T. (2005). Reinitiation of subduction and magmatic responses in SW Japan during Neogene time. *Geological Society of America Bulletin*, *117*(7-8), 969–986. https://doi.org/10.1130/B25565.1

Kita, I., Asakawa, Y., Yuri, T., Yasui, M., Shimoike, Y., Yamamoto, M., et al. (2012). Rifting of Kyushu, Japan, based on the fault-controlled concurrent eruption of oceanic island basalt-type and island arc-type lavas. *Bulletin of Volcanology*, *74*(5), 1121–1139. https://doi.org/10.1007/s00445-012-0587-z

Kotaki, A., Katoh, S., & Kitani, K. (2011). Correlation of Middle Pleistocene crystal-rich tephra layers from Daisen Volcano, southwest Japan, based on the chemical composition and refractive index of mafic minerals. *Quaternary international*, *246*(1-2), 105–117. https://doi.org/10.1016/j.quaint.2011.08.014

Kuritani, T., Yokoyama, T., Kobayashi, K., & Nakamura, E. (2003). Shift and rotation of composition trends by magma mixing: 1983 eruption at Miyake-jima Volcano, Japan. *Journal of Petrology*, *44*(10), 1895–1916. https://doi.org/10.1093/petrology/egg063

Kutterolf, S., Schindlbeck, J. C., Robertson, A. H. F., Avery, A., Baxter, A. T., Petronotis, K., & Wang, K. L. (2018). Tephrostratigraphy and provenance from IODP Expedition 352, Izu-Bonin Arc: Tracing tephra sources and volumes from the Oligocene to Recent. *Geochemistry, Geophysics, Geosystems*, *19*, 150–174. https://doi.org/10.1002/2017GC007100

Lowe, D. J. (2011). Tephrochronology and its application: A review. *Quaternary Geochronology*, *6*(2), 107–153. https://doi.org/10.1016/j.quageo.2010.08.003

Machida, H. (1999). The stratigraphy, chronology and distribution of distal marker-tephras in and around Japan. *Global and Planetary Change*, *21*(1-3), 71–94. https://doi.org/10.1016/S0921-8181(99)00008-9

Machida, H. (2002). Volcanoes and tephras in the Japan area. *Global Environmental Research -English Edition*, *6*(2), 19–28.

Machida, H., & Arai, F. (1992). *Atlas of tephra in and around Japan*. Tokyo, 276p: University of Tokyo Press. (in Japanese)

Machida, H., & Arai, F. (2003). *Atlas of tephra in and around Japan*, (revised ed.). Tokyo, 336p: University of Tokyo Press. (in Japanese)

Mahony, S. H., Sparks, R. S. J., Wallace, L. M., Engwell, S. L., Scourse, E. M., Barnard, N. H., et al. (2016). Increased rates of large-magnitude explosive eruptions in Japan in the late Neogene and Quaternary. *Geochemistry, Geophysics, Geosystems*, *17*, 2467–2479. https://doi.org/10.1002/2016GC006362

Miller, D. M., Goldstein, S. L., & Langmuir, C. H. (1994). Cerium/lead and lead isotope ratios in arc magmas and the enrichment of lead in the continents. *Nature*, *386*(6471), 514. https://doi.org/10.1038/368514a0

Miyoshi, M., Shibata, T., Yoshikawa, M., Sano, T., Shinmura, T., & Hasenaka, T. (2011). Genetic relationship between post-caldera and caldera-forming magmas from Aso volcano, SW Japan: Constraints from Sr isotope and trace element compositions. *Journal of mineralogical and petrological sciences*, *106*(2), 114–119. https://doi.org/10.2465/jmps.101021b

Moriwaki, H., Westgate, J. A., Sandhu, A. S., Preece, S. J., & Arai, F. (2008). New glass fission-track ages of Middle Pleistocene tephras on Yakushima Island, southern Japan. *Quaternary International*, *178*(1), 128–137. https://doi.org/10.1016/j.quaint.2006.11.013

Münker, C., Weyer, S., Scherer, E., & Mezger, K. (2001). Separation of high field strength elements (Nb, Ta, Zr, Hf) and Lu from rock samples for MC-ICPMS measurements. *Geochemistry, Geophysics, Geosystems*, *2*(12). https://doi.org/10.1029/2001GC000183

Nishizawa, F., & Suzuki, T. (2016). Re-examination of previous correlation of distal Ks5 Tephra and proximal Oda pyroclastic flow deposits in South Kyushu, SW Japan. *Geographical Reports of Tokyo Metropolitan University*, *51*, 83–91.

Notsu, K., Arakawa, Y., & Kobayashi, T. (1990). Strontium isotopic characteristics of arc volcanic rocks at the initial stage of subduction in western, Japan. *Journal of volcanology and geothermal research*, *40*(3), 181–196. https://doi.org/10.1016/0377-0273(90)90120-5

Pearce, J. A., Kempton, P. D., Nowell, G. M., & Noble, S. R. (1999). Hf-Nd element and isotope perspective on the nature and provenance of mantle and subduction components in Western Pacific arc-basin systems. *Journal of Petrology*, *40*(11), 1579–1611. https://doi.org/10.1093/petroj/40.11.1579

Pearce, J. A., Thirlwall, M. F., Ingram, G., Murton, B. J., Arculus, R. J., & Van der Laan, S. R. (1992). 13. Isotopic evidence for the origin of boninites and related rocks drilled in the Izu-Bonin (Ogasawara) forearc, Leg 125. In *Proc. Ocean Drilling Program, Scientific Results*, (Vol. 125, pp. 237–261). College Station Texas: Ocean Drilling Program. https://doi.org/10.2973/odp.proc.sr.125.134.1992

Pin, C., & Zalduegui, J. F. S. (1997). Sequential separation of light rare-earth elements, thorium and uranium by miniaturized extraction chromatography: application to isotopic analyses of silicate rocks. *Analytica Chimica Acta*, *339*(1-2), 79–89. https://doi.org/10.1016/S0003-2670(96)00499-0

Pouchou, J. L., & Pichoir, F. (1984). 'PAP' (φ–ρ–ζ) correction procedure for improved quantitative microanalysis. In J. T. Armstrong (Ed.), *Microbeam Analysis*, (pp. 104–106). San Francisco, CA: San Francisco Press.

Pownall, J. M., Lister, G. S., & Spakman, W. (2017). Reconstructing subducted oceanic lithosphere by "reverse-engineering" slab geometries: The northern Philippine Sea Plate. *Tectonics*, *36*, 1814–1834. https://doi.org/10.1002/2017TC004686

Reagan, M. K., Ishizuka, O., Stern, R. J., Kelley, K. A., Ohara, Y., Blichert-Toft, J., et al. (2010). Fore-arc basalts and subduction initiation in the Izu-Bonin-Mariana system. *Geochemistry, Geophysics, Geosystems*, *11*, Q03X12. https://doi.org/10.1029/2009GC002871

Reagan, M. K., Pearce, J. A., Petronotis, K., Almeev, R., Avery, A. A., Carvallo, C., et al. (2015). Site U1439. In M. K. Reagan, J. A. Pearce, K. Petronotis, and the Expedition 352 Scientists (Eds.), *Izu-Bonin-Mariana Fore Arc. Proceedings of the International Ocean Discovery Program, 352*. College Station, TX: International Ocean Discovery Program. https://doi.org/10.14379/iodp.proc.352.103.2015

Schindlbeck, J. C., Kutterolf, S., Straub, S. M., Andrews, G. D., Wang, K. L., & Mleneck-Vautravers, M. J. (2018). One Million Years tephra record at IODP S ites U 1436 and U 1437: Insights into explosive volcanism from the Japan and Izu arcs. *Island Arc*, *27*(3). https://doi.org/10.1111/iar.12244

Schmidt, A. (2001). *Temporal and Spatial Evolution of the Izu Island Arc, Japan, in Terms of Sr-Nd-Pb Isotope Geochemistry, Doctoral Thesis* (81 pp.). Kiel: Christians-Albrecht-University.

Scudder, R. P., Murray, R. W., Schindlbeck, J. C., Kutterolf, S., Hauff, F., Underwood, M. B., & McKinley, C. C. (2016). Geochemical approaches to the quantification of dispersed volcanic ash in marine sediment. *Progress in Earth and Planetary Science*, *3*(1), 1–32. https://doi.org/10.1186/s40645-015-0077-y

Self, S. (2006). The effects and consequences of very large explosive volcanic eruptions. *Philosophical Transactions of the Royal Society of London A: Mathematical, Physical and Engineering Sciences*, *364*(1845), 2073–2097. https://doi.org/10.1098/rsta.2006.1814

Shibata, T., Suzuki, J., Yoshikawa, M., Kobayashi, T., Miki, D., & Takemura, K. (2013). Geochemical and Sr-Nd-Pb Isotopic Constraints on the Origin and Magmatic Evolution of Quaternary Lavas of Sakurajima Volcano, Southern Kyushu Island, Japan (< Special Section> Sakurajima Special Issue). *Bulletin of the Volcanological Society of Japan*, *58*(1), 43–58. https://doi.org/10.18940/kazan.58.1_43

Shibata, T., Yoshikawa, M., Ujike, O., Miyoshi, M., & Takemura, K. (Eds) (2014). Along-arc geochemical variations in Quaternary magmas of northern Kyushu Island, Japan, in Gómez-Tuena, A., Straub, S. M. and Zellmer, G. F. (eds) 2014. Orogenic Andesites and Crustal Growth. *Geological Society, London, Special Publications*, *385*(1), 15–29. https://doi.org/10.1144/SP385.13

Shinjo, R. (1998). Petrochemistry and tectonic significance of the emerged late Cenozoic basalts behind the Okinawa Troughs Ryukyu arc system. *Journal of Volcanology and Geothermal Research*, *80*(1), 39–53. https://doi.org/10.1016/S0377-0273(97)00042-5

Shinjo, R., Chung, S. L., Kato, Y., & Kimura, M. (1999). Geochemical and Sr-Nd isotopic characteristics of volcanic rocks from the Okinawa Trough and Ryukyu Arc: Implications for the evolution of a young, intracontinental back arc basin. *Journal of Geophysical Research*, *104*(B5), 10,591–10,608. https://doi.org/10.1029/1999JB900040

Shinjo, R., Woodhead, J. D., & Hergt, J. M. (2000). Geochemical variation within the northern Ryukyu Arc: magma source compositions and geodynamic implications. *Contributions to Mineralogy and Petrology*, *140*(3), 263–282. https://doi.org/10.1007/s004100000

Straub, S. M. (2003). The evolution of the Izu Bonin–Mariana volcanic arcs (NW Pacific) in terms of major element chemistry. *Geochemistry, Geophysics, Geosystems*, *4*(2), 1018. https://doi.org/10.1029/2002GC000357

Straub, S. M., Goldstein, S. L., Class, C., & Schmidt, A. (2009). Mid-ocean-ridge basalt of Indian type in northwest Pacific Ocean Basin. *Nature Geoscience*, *2*, 286–289. https://doi.org/10.1038/NGEO471

Straub, S. M., Goldstein, S. L., Class, C., Schmidt, A., & Gomez-Tuena, A. (2010). Slab and mantle controls on the Sr–Nd–Pb–Hf isotope evolution of the post 42 Ma Izu–Bonin volcanic arc. *Journal of Petrology*, *51*(5), 993–1026. https://doi.org/10.1093/petrology/egq009

Straub, S. M., Layne, G. D., Schmidt, A., & Langmuir, C. H. (2004). Volcanic glasses at the Izu arc volcanic front: New perspectives on fluid and sediment melt recycling in subduction zones. *Geochemistry, Geophysics, Geosystems*, *5*, Q01007. https://doi.org/10.1029/2002GC000408

Straub, S. M., Woodhead, J. D., & Arculus, R. J. (2015). Temporal evolution of the Mariana Arc: Mantle wedge and subducted slab controls revealed with a tephra perspective. *Journal of Petrology*, *56*(2), 409–439. https://doi.org/10.1093/petrology/egv005

Tanaka, T., Togashi, S., Kamioka, H., Amakawa, H., Kagami, H., Hamamoto, T., et al. (2000). JNdi-1: A neodymium isotopic reference in consistency with LaJolla neodymium. *Chemical Geology*, *168*(3-4), 279–281. https://doi.org/10.1016/S0009-2541(00)00198-4

Tani, K., Fiske, R. S., Tamura, Y., Kido, Y., Naka, J., & Shukuno, H. (2008). Sumisu volcano Izu-Bonin arc Japan: site of a silicic caldera-forming eruption from a small open-ocean island. *Bulletin of Volcanology*, *70*(5), 547–562. https://doi.org/10.1007/s00445-007-0153-2

Tatsumi, Y., Suzuki-Kamata, K., Matsuno, T., Ichihara, H., Seama, N., Kiyosugi, K., et al. (2018). Giant rhyolite lava dome formation after 7.3 ka supereruption at Kikai caldera, SW Japan. *Scientific Reports*, *8*(1), 2753. https://doi.org/10.1038/s41598-018-21066-w

Taylor, R. N., & Nesbitt, R. W. (1998). Isotopic characteristics of subduction fluids in an intra-oceanic setting, Izu–Bonin Arc, Japan. *Earth and Planetary Science Letters*, *164*(1), 79–98. https://doi.org/10.1016/S0012-821X(98)00182-4

Terakado, Y., Shimizu, H., & Masuda, A. (1988). Nd and Sr isotopic variations in acidic rocks formed under a peculiar tectonic environment in Miocene Southwest Japan. *Contributions to Mineralogy and Petrology*, *99*(1), 1–10. https://doi.org/10.1007/BF00399360

Todt, W., Clift, R. A., Hanser, A., & Hofmann, A. W. (1996). Evaluation of a 202Pb-205Pb double spike for high precision lead analysis. In A. Basu, & S. R. Hart (Eds.), *Earth Processes: Reading the Isotopic Code: Geophysical Monograph*, (Vol. 95, pp. 429–437). Washington, DC: American Geophysical Union. https://doi.org/10.1029/GM095p0429

Tollstrup, D., Gill, J., Kent, A., Prinkey, D., Williams, R., Tamura, Y., & Ishizuka, O. (2010). Across-arc geochemical trends in the Izu-Bonin arc: Contributions from the subducting slab, revisited. *Geochemistry, Geophysics, Geosystems*, *11*, Q01X10. https://doi.org/10.1029/2009GC002847

Torii, M., & Oda, M. (2001). Correlation of the Izaku Pyroclastic Flow Deposit in Kagoshima Prefecture with tuff bed intercalated in the Miyazaki Group: The eruption age of the Izaku-Hisamine tephra based on integrated stratigraphy of the Miyazaki Group and it significance. *Journal of Geological Society of Japan*, *107*, 379–391 (in Japanese with English abstract). https://doi.org/10.5575/geosoc.107.379

Torii, M., Oda, M., & Itaya, T. (2000). K-Ar dating of tuff beds intercalated in the Miyazaki Group, Kyushu, Japan. *Bulletin of the Volcanological Society of Japan*, *45*, 131–148 (in Japanese with English abstract. https://doi.org/10.18940/kazan.45.3_131

Tsuji, T., Ikeda, M., Furusawa, A., Nakamura, C., Ichikawa, K., Yanagida, M., et al. (2017). High resolution record of Quaternary explosive volcanism recorded in fluvio-lacustrine sediments of the Uwa basin, southwest Japan. *Quaternary International*, *471*(B), 278–297. https://doi.org/10.1016/j.quaint.2017.10.016

Vervoort, J. D., & Blichert-Toft, J. (1999). Evolution of the depleted mantle; Hf isotope evidence from juvenile rocks through time. *Geochimica et Cosmochimica Acta*, *63*(3-4), 533–556. https://doi.org/10.1016/S0016-7037(98)00274-9

Weis, D., Kieffer, B., Hanano, D., Nobre Silva, I., Barling, J., Pretorius, W., et al. (2007). Hf isotope compositions of US Geological Survey reference materials. *Geochemistry, Geophysics, Geosystems*, *8*, Q06006. https://doi.org/10.1029/2006GC001473

Weis, D., Kieffer, B., Maerschalk, C., Barling, J., de Jong, J., Williams, G. A., et al. (2006). High-precision isotopic characterization of USGS reference materials by TIMS and MC-ICP-MS. *Geochemistry, Geophysics, Geosystems*, *7*, Q08006. https://doi.org/10.1029/2006GC001283

White, W. M., Albarède, F., & Télouk, P. (2000). High-precision analysis of Pb isotope ratios using multi-collector ICP-MS. *Chemical Geology*, *167*, 257–270. https://doi.org/10.1016/S0009-2541(99)00182-5

White, W. M., & Patchett, J. (1984). Hf-Nd-Sr isotopes and incompatible element abundances in island arcs: implications for magma origins and crust-mantle evolution. *Earth and Planetary Science Letters*, *67*(2), 167–185. https://doi.org/10.1016/0012-821X(84)90112-2

Woodhead, J. D. (1989). Geochemistry of the Mariana arc (western Pacific): Source composition and processes. *Chemical Geology*, *76*(1-2), 1–24. https://doi.org/10.1016/0009-2541(89)90124-1

Wu, J., Suppe, J., Lu, R., & Kanda, R. (2016). Philippine Sea and East Asian plate tectonics since 52 Ma constrained by new subducted slab reconstruction methods. *Journal of Geophysical Research: Solid Earth*, *121*, 4670–4741. https://doi.org/10.1002/2016JB012923

Yamamoto, T., Kudo, T., & Isizuka, O. (2018). Temporal variations in volumetric magma eruption rates of Quaternary volcanoes in Japan. *Earth, Planets and Space*, *70*(1), 1–12. https://doi.org/10.1186/s40623-018-0849-x

Yogodzinski, G. M., Bizimis, M., Hickey-Vargas, R., McCarthy, A., Hocking, B. D., Savov, I. P., et al. (2018). Implications of Eocene-age Philippine Sea and forearc basalts for initiation and early history of the Izu-Bonin-Mariana arc. *Geochimica et Cosmochimica Acta*, *228*, 136–156. https://doi.org/10.1016/j.gca.2018.02.047